

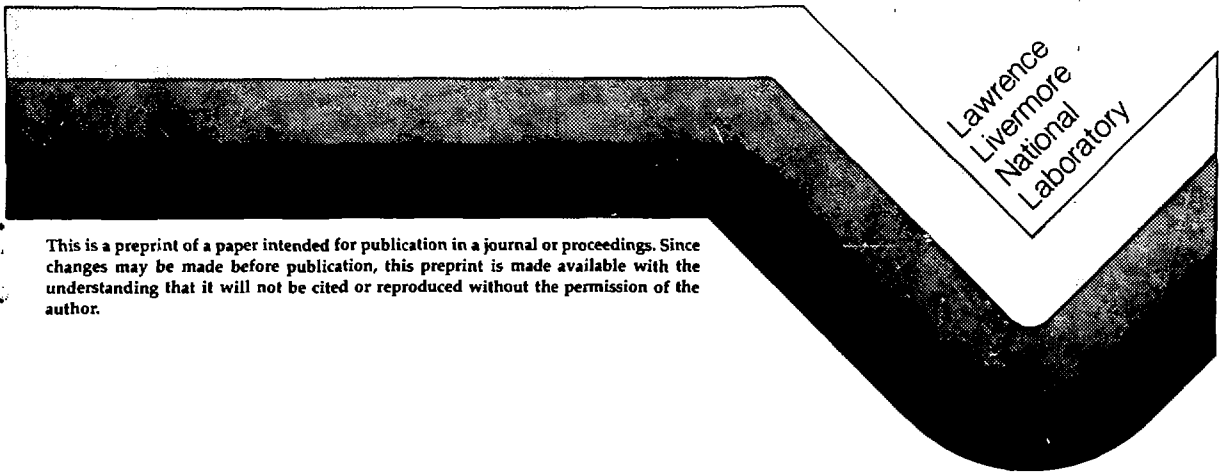
CONF - 831203 -- 13

**DESIGN OF A SEPARATOR/NEUTRALIZER TO LIMIT  
IMPURITIES AND NON-PRIMARY SPECIES IN THE  
MIRROR FUSION TEST FACILITY**

A. I. Goldner

This paper was prepared for submittal to the  
IEEE 10th Symposium on Fusion Engineering,  
Philadelphia, PA, December 5-9, 1983.

November 30, 1983



This is a preprint of a paper intended for publication in a journal or proceedings. Since changes may be made before publication, this preprint is made available with the understanding that it will not be cited or reproduced without the permission of the author.

**MASTER**

DESIGN OF A SEPARATOR/NEUTRALIZER TO LIMIT IMPURITIES AND  
NON-PRIMARY SPECIES IN THE MIRROR FUSION TEST FACILITY\*

Alan T. Goldner  
Lawrence Livermore National Laboratory, University of California  
Livermore, CA 94550

Abstract

The optimum plasma for the tandem Mirror Fusion Test Facility (MFTF-B) at Lawrence Livermore National Laboratory (LLNL) is very sensitive to heavy contaminants, such as oxygen and metals. Unfortunately the current neutral beam sources generate not only high energy deuterium particles but also high energy oxygen particles. A new MFTF-B separator/neutralizer has been designed to filter out the unwanted oxygen and allow only primary species neutrals to reach the plasma.

Introduction

The separator/neutralizer utilizes the concept of magnetic-momentum separation of the various ionized energetic species. In most beams on MFTF-B (except the passing-particle barrier beam or P2B2), the primary species are 80-kV neutral particles. Bending the 80-kV deuterium ions  $9.2^\circ$  with a separator magnet as they leave the source allows only the 80-kV deuterium particles to exit through a properly placed aperture. The oxygen ions and any particle with an atomic number greater than two are bent very little by the separator magnet and thus hit above the aperture. The half- and third-energy ions of deuterium are bent more than  $9.2^\circ$  and therefore hit below the aperture.

We have completed a parametric analysis of the effect of varying three geometric aspects: the length of the neutralizer, the distance from the source to the magnet, and the pressure distribution along the neutralizer. Here we present our analysis and design details of the prototype neutralizer that will soon be tested at Lawrence Berkeley Laboratory (LBL) on the Neutral Beam Engineering Test Stand (NBETF).

The Contaminant Problem

Oxygen

Mathematical models and experimental evidence show that the oxygen level in a stream of high-energy-injected neutral particles of only 10 parts per million (ppm) can degrade the stability of the plasma. Most lower energy contaminants can be shielded from the central plasma by the low density plasma halo surrounding the central plasma in MFTF-B, but the halo is porous to high energy neutral particles such as oxygen. Experimental work at various laboratories has shown that the present generation of neutral beam sources produces between 0.1 and 1% high energy oxygen ions. These particles have been detected by both optical multichannel analyzers (OMA) and magnetic analyzers.

Getting the inside of the neutral beam source has been proposed as an effective means of limiting the oxygen accelerated by the ion source grids. However, this system has limitations where long pulse sources are involved because the gettering medium is saturated before 30 s have elapsed.

Low Energy Deuterium

Another constraint on the neutral beam source, also determined by the mathematical model, is the necessity for very high atomic fractions of the primary species. The most recent generation of neutral beam sources has a species mix of approximately 80% of 80-kV particles, 15% of 40-kV particles, and 5% of 27-kV particles. If, instead of only obtaining 80% of 80-kV particles, the fraction was increased to 98%, the necessary amount of 80-kV particles injected into the plasma would drop by more than half. This is an important fact because getting almost any particles into the transition region of MFTF-B is a difficult job due to geometric constraints.

In the following discussion we show how the separator/neutralizer can filter out most lower energy components of the deuterium beam and leave a beam with an 80-kV fraction of greater than 98%.

Separator/Neutralizer Concept

As noted, the basic concept of the separator/neutralizer is magnetic-momentum separation of the various ionized species produced by the plasma generator of the neutral beam source. Figure 1 shows the type and percentage of each particle. All but the 80-kV deuterium particles should be restrained from reaching the plasma.

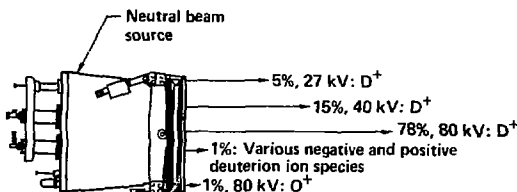


Fig. 1. Percent of deuterium and oxygen particles in a typical neutral beam source for MFTF-B.

In almost all cases the MFTF-B plasma target is approximately 1 m high and 9 m from the neutral beam source. By utilizing this fact and assuming a spatial distribution of the deuterium and oxygen particles, we calculated the angle by which the 80-kV deuterium particles should be separated from the normal angle. The correct angle of separation should allow no more than one particle of oxygen for every million particles of deuterium to intercept the plasma 9 m away. A magnet of sufficient field can bend the deuterium ions. By this method the light 80-kV deuterium ions are bent much more than the heavier 80-kV oxygen ions. This separation scheme is shown in Fig. 2.

An approximation of the uniform field necessary to bend the singly ionized particles is shown below [1]:

$$\text{Radius of curvature} = c \left[ \frac{(A)(K)^{1/2}}{B} \right] \quad (1)$$

where

C = constant,

\*Work performed under the auspices of the U.S. Department of Energy by the Lawrence Livermore National Laboratory under contract number W-7405-ENG-48.

249

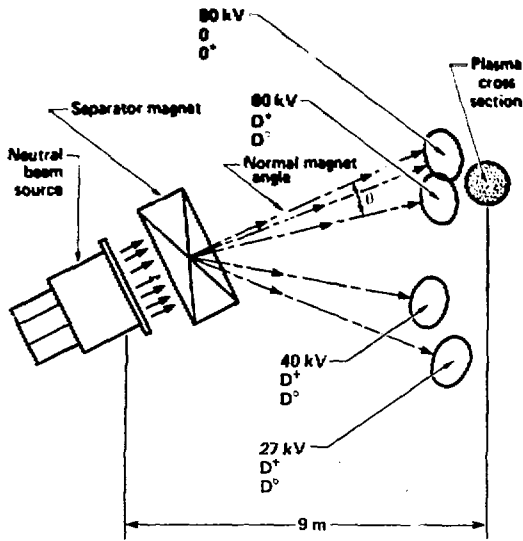


Fig. 2. Ion trajectories produced by a separator magnet.

- A = atomic mass number,
- K = Kinetic energy in eV,
- B = uniform field in G.

Equation (1) shows that the bending angle of two ions is a function of the atomic mass when the particle energy is equal. As seen in Fig. 2, the 40-kV and 27-kV particles are bent much more by the magnetic field than the 80-kV particles. Since the requirement for limiting oxygen is much stricter than for low energy deuterium, the separation between 80-kV oxygen and 80-kV deuterium is the controlling factor in the calculation of the separation angle. Furthermore, by separating the oxygen and deuterium enough to meet the 1-ppm limit, the 27-kV and 40-kV deuterium particles are separated from the 80-kV deuterium particles to meet the 98% fraction requirement.

Loss Problems

There are two conflicting design objectives in engineering a separator/neutralizer. One objective is a high pressure in the neutralizer section to keep the neutralizer length short (neutralization efficiency being a function of the integral of pressure and distance). The second objective is to keep the length from the source exit grid to the separator magnet at a very low pressure. This low pressure is needed so that the deuterium ions leaving the source exit grid do not neutralize before they reach the separator magnet. Neutrals entering the magnetic field are not bent and, hence, will not have the correct trajectory to reach the plasma. The ions entering the field must continue to be ions throughout the magnetic field to assure the correct bending radius.

A conceptual design emerged from these constraints and requirements; Fig. 3 illustrates the necessary components of the design, including the separator magnet, neutralizer, and source hat. Each chamber of the separator/neutralizer has its own set of defining characteristic equations relating pressure versus source efficiency. (Source efficiency shall be defined as the fraction of 80-kV neutral particles on the target

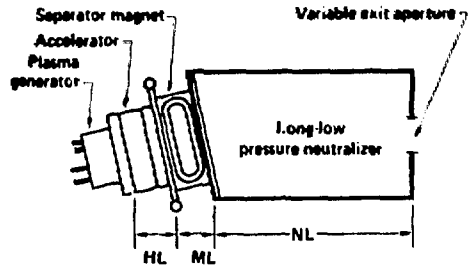


Fig. 3. Basic components of the separator/neutralizer planned for MFTF-B, denoting hat length (HL), magnet length (ML), and neutralizer length (NL).

plasma as compared with the total extracted current.) The following discussions outline these equations in detail.

Defining Equations of Source Hat

We define the "source hat" as the distance from the source exit grid to the beginning of the field of the separator magnet. Specifically, the hat distance consists of the space taken up by the electric insulators separating the 80-kV source input from ground. The basic efficiency equation is just the inverse of the efficiency equation for a neutralizer. In this chamber the fraction of particles that leave the chamber as neutrals are lost--due to effects of the bending magnet--and must be minimized.

Equation (2) indicates the percent of 80-kV particles entering the separator magnet as ions:

$$\frac{80\text{-kV ions}}{\text{All } 80\text{-kV particles}} = 1 - \left( \frac{\text{Neutral-ization fraction} \times \text{Neutral-ization efficiency}}{\text{fraction efficiency}} \right), \quad (2)$$

where

$$\text{Neutralization fraction} = \frac{\sigma_{01}}{\sigma_{01} + \sigma_{10}} = F_0 ;$$

$$\text{Neutralization efficiency} = 1 - \exp[-KP(HL)]$$

and

$$\sigma_{01} = \text{cross section of } D^0 \text{ for ionization in } D_2 \text{ gas,}$$

$$\sigma_{10} = \text{cross section of } D^0 \text{ for neutralization in } D_2 \text{ gas,}$$

$$K = \text{constant} \times (\sigma_{01} + \sigma_{10}),$$

$$P = \text{hat section pressure in Torr,}$$

$$HL = \text{hat section length in cm.}$$

Therefore, the source hat equation is

$$\frac{80\text{-kV ions}}{\text{All } 80\text{-kV particles}} = 1 - F_0 \{1 - \exp[-KP(HL)]\}. \quad (3)$$

For 80-kV deuterium particles this equation is

$$\frac{80\text{-kV ions}}{\text{All } 80\text{-kV particles}} = 1 - 0.625 \{1 - \exp[-13.3(P)(HL)]\}. \quad (4)$$

Defining Equations for the Separator Magnet Section

The apparent length of the magnet used in the equation is assumed to be twice the pole width; this

is not necessarily the actual dimension of the hardware itself.

The neutral particles that pass into the separator magnet from the source hat region are not bent by the field and, hence, are lost to the total of 80-kV particles intercepting the plasma. Unlike Eq. (2) for the hat region, the magnet region equation below shows a loss of any particle that neutralizes even once. A particle must remain an ion throughout the traverse through the magnetic field to receive the correct trajectory to bring it into the plasma. Therefore, the loss equation uses the ionic fraction rather than the equilibrium fraction:

$$\frac{\text{Fraction of ions remaining as ions}}{\text{Total ions entering magnet}} = 1 - \exp[-K_0 P(HL)], \quad (5a)$$

where

$$K_0 = \text{Constant} \times \sigma_{10};$$

HL = Apparent magnet length measured in cm.

For 80-kV ions the equation becomes:

$$\frac{\text{Fraction of ions remaining as ions}}{\text{Total ions entering magnet}} = 1 - \exp[-8.31(P)(HL)]. \quad (5b)$$

#### Defining Equations for the Neutralizer Section

The neutralizer section extends from the edge of the magnetic field of the separator magnet (as defined before) to the exit aperture of the neutralizer itself. The particles that leave the neutralizer as ions are lost to the plasma. We can express this as

$$\frac{\text{Particles leaving as neutrals}}{\text{Particles entering as ions}} = \frac{\text{Equilibrium fraction}}{\text{Neutralizer efficiency}}; \quad (6a)$$

or

$$\frac{\text{Particles leaving as neutrals}}{\text{Particles entering as ions}} = F_0 \{1 - \exp[-KP(NL)]\}, \quad (6b)$$

where NL = neutralizer length in cm. For 80-kV deuterium, we can rewrite the equation as

$$\frac{\text{Particles leaving as neutrals}}{\text{Particles entering as ions}} = 0.625 \{1 - \exp[-13.3(P)(NL)]\}. \quad (6c)$$

The total efficiency equation of all the loss equations multiplied together becomes

$$\frac{\text{Neutrals on the plasma}}{\text{Total current extracted}} = F_{80} F_0 \{1 - \exp[-KP(NL)]\} \times \{1 - F_0 + F_0 \exp[-KP(HL)]\} \times \{\exp[-K_0 P(HL)]\}, \quad (7)$$

where

$$F_{80} = \text{fraction of total current extracted as 80-kV ions.}$$

#### Parametric Evaluation

Using Eq. (7), we can perform a parametric analysis to determine the most efficient geometry. First we

varied the length of one chamber and kept the other two constant. We determined the length of the first chamber through past beamline experience. Then we calculated the pressure ranges from 0 to  $10^{-4}$  Torr, again utilizing previous beamline experience to bracket the pressure range. The pressures in all chambers were assumed equal to one another for each efficiency calculation. Although in actual practice the pressure would vary from the exit grid to the end of the neutralizer, an isobaric assumption is adequate. As a check, the pressures in the chambers were chosen so that the neutralizer pressure was less than the hat pressure by an order of magnitude. Because this change did not affect the trend analysis, this complication was dropped.

Figures 4a-c show how the efficiency changed as the lengths of the three chambers—neutralizer, magnet, and source hat—were varied along with their pressure. The following discussion details our studies.

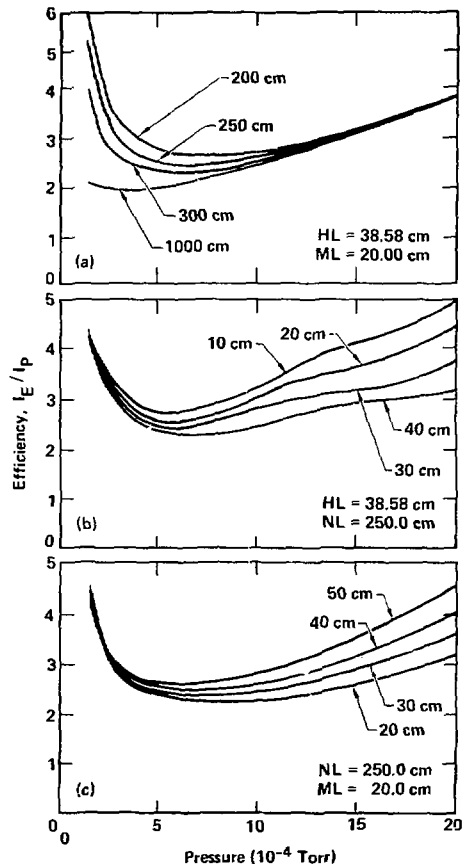


Fig. 4. Efficiency curves in our parametric analysis: (a) varying the neutralizer length (NL); (b) varying the effective magnet length (ML); (c) varying the source hat length (HL).

#### Neutralizer Length vs Pressure

Figure 4a depicts the neutralizer length versus pressure efficiency curve. As shown, at very low pressure the overall efficiency drops drastically because the neutralizer section efficiency goes to zero at low pressures. A neutralizer length of 1000 cm is much

more efficient than a 200-cm-long one at low pressure. Conversely, a 300-cm-long neutralizer is not appreciably better than a 200-cm-long neutralizer. Space limitations in the MBTF-B concrete vault dictate a short neutralizer. Thus, we chose a 250-cm-long neutralizer and used this length in the rest of our parametric analysis.

#### Magnet Length vs Pressure

The curve relating magnet length and chamber pressure to efficiency is shown in Fig. 4b. The magnet length is the effective magnet length, that is, the region of the magnet where the field strength is high enough to affect the ion trajectory appreciably. When designing a magnet, this distance is usually twice the pole width (if field clamps are used).

From the curve it is obvious to see that a magnet having the shortest apparent length is desirable. Specifically, the less time the ion traverses the field, the less chance it has for gaining an electron and neutralizing. Magnet pole lengths are limited by the bending radius of the copper conductor composing the coils. The other nonmechanical factor limiting pole length is the problem of increasing fringe fields with decreasing pole length. Since the ion needs a constant integral of magnetic field times length, decreasing the length necessitates an increase in the field. The source cannot operate in an environment of more than 1 G; therefore, the fringe field must be limited to less than that at the exit grid. Again,

from past experience with magnet design, we determined that a 20-cm-magnet was a reasonable length for our initial calculations.

#### Source Hat Length vs Pressure

Figure 4c relates the source hat length and pressure to efficiency. For hat lengths between 20 and 50 cm, the efficiency does not appreciably decrease with length. Therefore, a minimum hat length of 32 cm was chosen for analysis because it is the average distance between the source exit grid and the bolting flange for both the LBL and Oak Ridge National Laboratory (ORNL) prototype long-pulse sources.

#### Prototype Design

To validate previous calculations that show the separator/neutralizer will purify the beam of oxygen and low energy deuterium, a full scale prototype has been built. The separator/neutralizer must accept either the LBL 10 cm x 40 cm, 4-MW, 30-s source or the ORNL 13 cm x 43 cm, 4-MW, 30-s source. Although both of these sources are prototypes, the production sources should be very similar. When initial testing of the device is complete, the prototype separator/neutralizer will be installed in the Neutral Beam Engineering Test Stand (NBETF) at LBL. The neutralizer section will be in the vacuum tank of the NBETF, and the magnet/source will be on the outside of the tank. This arrangement is shown in Fig. 5.

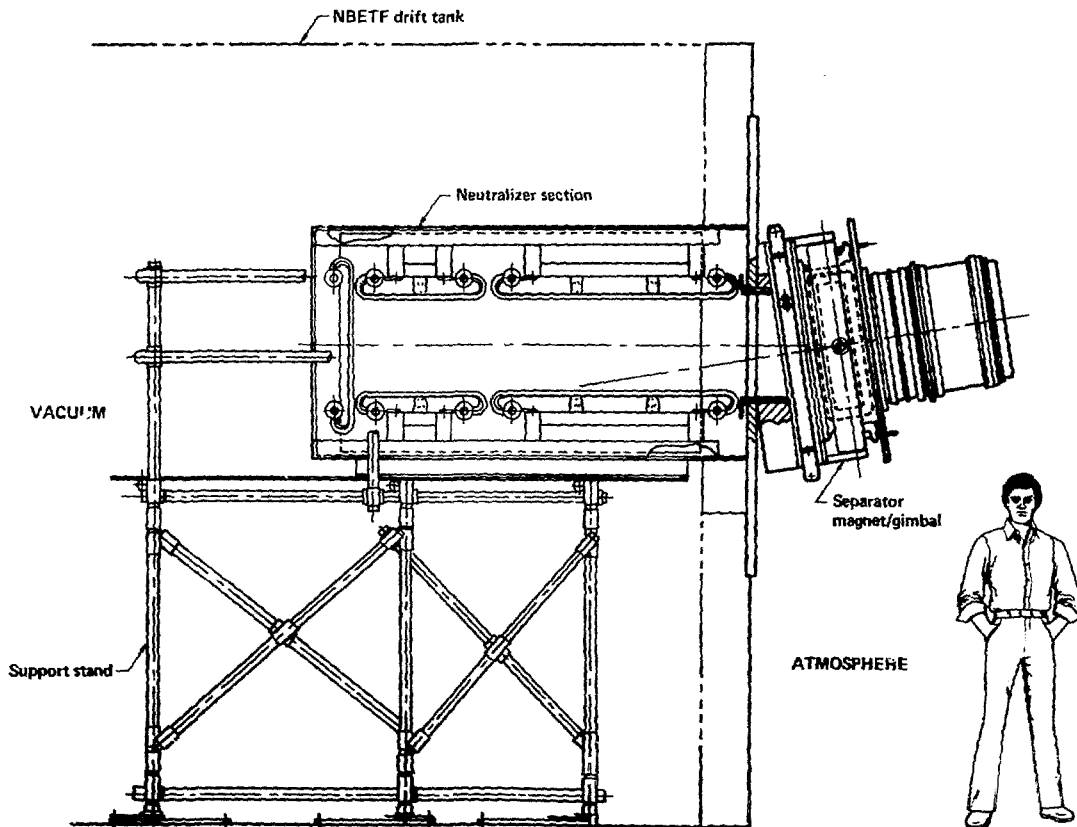
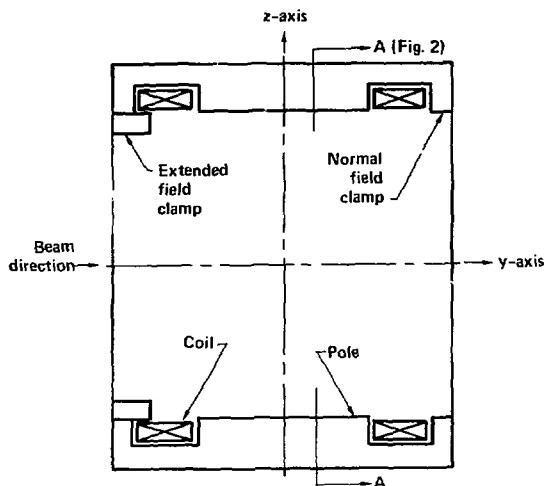


Fig. 5. Layout of the separator/neutralizer installed in the Neutral Beam Engineering Test Stand at Lawrence Berkeley Laboratory.

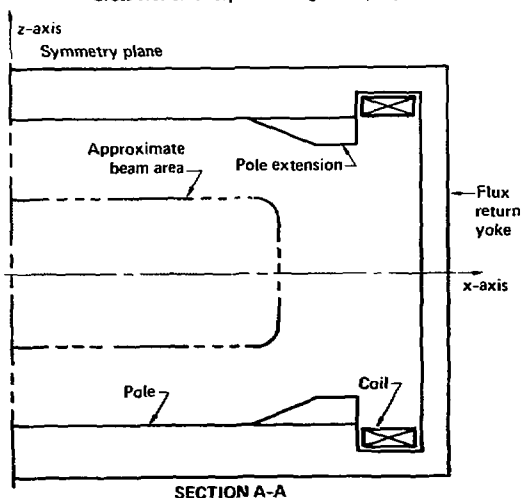
### Separator Magnet Design

The separator magnet is a conventional iron-dominated dipole with water-cooled coils. It is fabricated with poles and field clamps integral to the yoke. The yoke is a one-piece weldment that functions as a portion of the system vacuum chamber in addition to its normal magnetic function.

It was desirable in our design to have a large gap-to-pole-width ratio to reduce gas pressure on the upstream or negative-y side of the magnet inside the neutralizer (Fig. 6). In addition, a limitation on the fringe field amplitude exists; that is, the fringe field could not exceed 1 G at the beam source. To avoid premature neutralization of particles, it was necessary that the separator magnet be relatively close to the source. Thus, three simultaneously counter-acting features--large gap, low fringe field, and close proximity to the source--were specified for this magnet.



Cross-section of separator magnet in y-z plane



SECTION A-A

Fig. 6. Cross section of the separator magnet in the x-z plane.

To accomplish this design, we employed the Poisson group of computer codes [1] in conjunction with the Superbeam code group [2]. The Poisson group was used to analyze two-dimensional representations of the magnet, whereas the superbeam codes were used to observe effects on the beam pattern caused by modifications to the magnet as well as to model the overall beam system. Vector potential maps from the Poisson group were input to Superbeam to develop a representation of a dipole field in the system. These code groups were principally developed by Halbach, Holtzinger, and Harnett, all (or formerly) of LBL.

Initial models of the dipole were created with conventional field clamps (Fig. 6). These field clamps worked as expected to limit the fringe fields. An extension to the normal field clamp on the upstream side further reduced the fringe field. Thus, a pole-to-pole-gap dimension of 25 cm was possible while maintaining fringe fields small enough to allow reasonable proximity to the source.

We examined various pole widths using the Poisson-Superbeam groups. After observing beam control and focusing effects, we chose a 14-cm pole width. As seen in Fig. 6, our final model is a narrow pole, large gap, dipole magnet with a reduced upstream fringe field that can be positioned relatively close to the beam source.

A major interface constraint limited the width of the magnet in the x-direction (Fig. 2). This obstacle was important since the magnet is used in conjunction with a large cross section source. To improve the field consistency across the magnet aperture in the x-direction, extensions to the poles were placed at the ends. These can be seen in Fig. 6. These wedge-like shapes were based on more complex shapes obtained through a careful computer optimization of another dipole magnet. Two-dimensional modeling of this feature significantly improved the field consistency in the extremes of the magnet aperture.

The separator magnet represents a somewhat complicated and detailed design carried out with a high degree of confidence by computer modeling. No prototyping or testing of physical models was required in this development process.

### Neutralizer Design

The neutralizer section must not only provide a high density medium for the ions to reach equilibrium but must also absorb all the power of the beam that does not exit at the prescribed  $9.2^\circ$  angle. There are three main components of the power impinging on the neutralizer. The first is the 80-kV, 40-kV, and 27-kV ions that neutralize in the source hat region and are not bent by the separator magnet. The second component is those particles entering the magnet as ions but which neutralize during their passage through the magnetic field and, hence, do not exit at a  $9.2^\circ$ . The third component is the 27-kV and 40-kV deuterium ions that remain as ions. The trajectories of all three are shown in Fig. 2.

Referring to the first component, the equation for the 80-kV, 40-kV, and 20-kV particles that enter the magnetic field as neutrals is

$$P_w = (X_A) \left[ (X_N F_F) 80 \times 10^3 + (2Y_N F_H) 40 \times 10^3 + (3Z_N F_D) 27 \times 10^3 \right], \quad (8)$$

where

$X_A$  = value of extracted amperes (A),

$X$  = fraction of 80-kV particles,

$Y$  = fraction of 40-kV particles,

- $Z$  = fraction of 27-kV particles,  
 $N$  = neutralizer efficiency,  
 $F$  = equilibrium fraction.

Subscripts: F = full-energy at 80 kV,  
 H = half-energy at 40 kV,  
 T = third-energy at 27 kV.

The power of the particles that enter the field as ions but are neutralized sometime during their path through the magnetic field is shown below:

$$P_W = X_{MF} [(XN_{FF}) (80 \times 10^3) + X_{MH} [(2YN_{HH}) (40 \times 10^3) + X_{MT} [(3ZN_{TT}) (27 \times 10^3)], \quad (9)$$

where

- $X_{MF}$  = total A entering magnets as ions =  $X_A$  - full-energy ions neutralized in the hat region,  
 $X_{MH}$  = total A entering magnets as ions =  $X_A$  - half-energy ions neutralized in the hat region,  
 $X_{MT}$  = total A entering magnets as ions =  $X_A$  - third-energy ions neutralized in the hat region,  
 $E$  = ionic cross section  $\{1 - \exp \{-K_O(ML)P\}\}$ ,  
 $K_F^O = 8.31$ ,  
 $K_H^O = 19.44$ ,  
 $K_T^O = 25.92$ .

The power of these particles as a function of length is shown in Fig. 7.

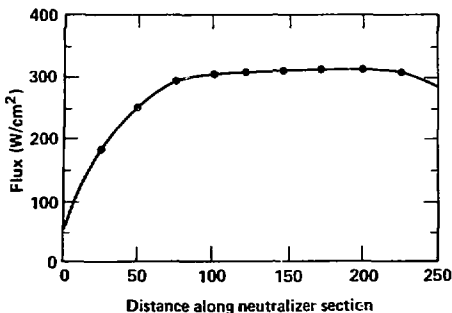


Fig. 7. Power deposited on the centerline of the neutralizer bottom shown as a function of length. We assumed source parameters as follows: extracted A = 50; V = 6 Torr l/s (excess gas); exit aperture conductance = 15000 l/s; species fraction: 80 kV = 0.80, 40 kV = 0.15, and 27 kV = 0.05.

Finally, there are the 27-kV and 40-kV particles that remain as ions through the magnet. These ions are bent more than  $9.2^\circ$  and proceed to the bottom of the neutralizer. The equation for this third component is

$$P_W = (X_{PH}) N_{H1} \{1 - F_{H1} + F_{H1} \exp \{-K_{H1}P(HL)\}\} \times (\exp \{-K_{H1}S(ML)\}) (40 \times 10^3) + (X_{MT}) N_T \{1 - F_T + F_T \exp \{-K_T P(HL)\}\} \times (\exp \{-K_T OP(ML)\}) (27 \times 10^3). \quad (10)$$

(The oxygen ions and neutrals add negligible power to the dumps and will be neglected.)

**High-Heat-Flux Panels:** For the neutralizer high-heat-flux panels (dumps) we selected arrays of internally finned copper tubes with a nominal  $2 \text{ kW/cm}^2$  rating for long life. However, all areas of the panels should have a considerably lower loading because of the extreme angle of the dumps with respect to the beam. Another pair of high-heat-flux panels is used at the exit of the neutralizer to protect the exit aperture. Table 1 shows the thermal and flow characteristics for these panels.

Table 1. Major characteristics of the high-heat-flux panels.

	Flow (gpm)	Peak flux ( $\text{kW/cm}^2$ )	Total flux (kW)	Temp. rise ( $^\circ\text{C}$ )
Top panels	110	0.320	500	17.0
Bottom panels	110	0.015	23.4	<1.0
Exit panels	80	0.100	50	5.0

**Tank Lining:** To protect the aluminum skin of the neutralizer tank, water-cooled stainless-steel pillowed panels line the walls. These panels protect the wall from particles with unknown trajectories.

**Gimbal Design:** The gimbal/magnet/valve assembly is shown in Fig. 5. The main design feature of the assembly is the positioning of copper cooling panels along the assembly walls. These panels are placed anywhere a surface has a "view" of the exit grid of the source.

#### Vacuum Calculations

Our vacuum analysis used the preliminary design as a guide for conductance calculations. The results, shown in Fig. 8, indicate that the efficiency of the separator/neutralizer can be increased by tailoring the exit conductance of the neutralizer to the input gas of the neutralizer. Since sources can run at most 50% efficiency (50% of all input gas is ionized), there is always a ready supply of  $D_2$  gas for neutralization. Decreasing the conductance increases the pressure in the magnet/hat regions, which is unfavorable; however, at the same time this increases the pressure in the neutralizer section, which is favorable. There is a best exit conductance for each gas input. In some instances additional gas may be injected into the neutralizer to increase neutralizer efficiency.

Our "as built" vacuum calculations differ from the preliminary design vacuum calculations in only one respect. The aperture through the magnet is not as great as the preliminary design, and therefore the conductance is less. In the final design a heat shield has been added to the inside of magnet to protect it from high energy particles coming off the exit grid at high angles. This decreases the prototype's efficiency by 23% from our earlier calculations.

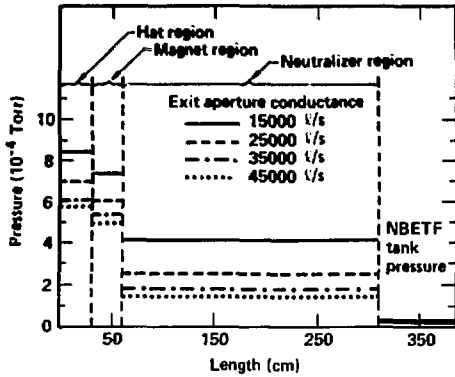


Fig. 8. Pressure distribution along the separator/neutralizer. We assumed  $V = 6$  Torr l/s (excess gas).

#### Conclusion

Mathematical modeling shows that a separator/neutralizer can limit neutral beam contaminants. We

have performed a preliminary design as well as a parametric analysis of neutralizer geometry. In addition, a prototype separator/neutralizer has been built and will soon undergo testing at LBL. The proof-of-principle test will use either an LBL or ORNL 4.0-MW source, and the individual test will last up to 30 s. Any future production model must have an increased magnet aperture so that its efficiency will approach that of our preliminary design.

#### Acknowledgment

We thank L. Dilgard for the very innovative prototype design and J. Fabyan for fabricating a prototype that seemed to resist assembly.

#### References

- [1] A. Winslow, "Numerical Solutions to Quasi-Linear Poisson Equations in a Nonuniform Triangular Mesh," *J. Comp. Phys.*, vol. 2, 149-172.
- [2] G. Harnett, "Beam Codes Users' Guide," Lawrence Berkeley Laboratory, Berkeley, CA, Draft (1983).

### DISCLAIMER

This report was prepared as an account of work sponsored by an agency of the United States Government. Neither the United States Government nor any agency thereof, nor any of their employees, makes any warranty, express or implied, or assumes any legal liability or responsibility for the accuracy, completeness, or usefulness of any information, apparatus, product, or process disclosed, or represents that its use would not infringe privately owned rights. Reference herein to any specific commercial product, process, or service by trade name, trademark, manufacturer, or otherwise does not necessarily constitute or imply its endorsement, recommendation, or favoring by the United States Government or any agency thereof. The views and opinions of authors expressed herein do not necessarily state or reflect those of the United States Government or any agency thereof.

#### DISCLAIMER

This document was prepared as an account of work sponsored by an agency of the United States Government. Neither the United States Government nor the University of California nor any of their employees, makes any warranty, express or implied, or assumes any legal liability or responsibility for the accuracy, completeness, or usefulness of any information, apparatus, product, or process disclosed, or represents that its use would not infringe privately owned rights. Reference herein to any specific commercial products, process, or service by trade name, trademark, manufacturer, or otherwise, does not necessarily constitute or imply its endorsement, recommendation, or favoring by the United States Government or the University of California. The views and opinions of authors expressed herein do not necessarily state or reflect those of the United States Government thereof, and shall not be used for advertising or product endorsement purposes.